Separation Science and Technology
Publication details, including instructions for authors and subscription information:
http://www.informaworld.com/smpp/title~content=t713708471

Effects of Heat-Transfer Coefficients on Thermal Dynamics in a Near-Adiabatic Fixed Bed

Hyungwoong Ahn[a]; Min-Bae Kim[b]; Chang-Ha Lee[b]
[a] Department of Chemical Engineering, University College London, London, England [b] Department of Chemical Engineering, Yonsei University, Seodaemun-gu, Seoul, Korea

Online publication date: 08 July 2010

To cite this Article Ahn, Hyungwoong , Kim, Min-Bae and Lee, Chang-Ha(2004) 'Effects of Heat-Transfer Coefficients on Thermal Dynamics in a Near-Adiabatic Fixed Bed', Separation Science and Technology, 39: 11, 2627 — 2654
To link to this Article: DOI: 10.1081/SS-200026757
URL: http://dx.doi.org/10.1081/SS-200026757

SEPARATION SCIENCE AND TECHNOLOGY
Vol. 39, No. 11, pp. 2627–2654, 2004

Effects of Heat-Transfer Coefficients on Thermal Dynamics in a Near-Adiabatic Fixed Bed

Hyungwoong Ahn,[1] Min-Bae Kim,[2] and Chang-Ha Lee[2,*]

[1]Department of Chemical Engineering, University College London, London, England
[2]Department of Chemical Engineering, Yonsei University, Seoul, Korea

ABSTRACT

Experimental and theoretical studies were performed to investigate thermal dynamics in a fixed bed. The near-adiabatic beds packed with virgin zeolite 13X and water-saturated zeolite 13X were heated with hot nitrogen. The effect of the heat-transfer coefficient between the gas and adsorbed phases, h_s, on thermal dynamics was elucidated by a comparison of the thermally heterogeneous and homogeneous models. If h_s is obtained from a proper correlation, the prediction of thermal dynamics by the homogeneous model is the same as that by the heterogeneous model. The heat-transfer coefficient at the inner wall, h_i, in the

*Correspondence: Chang-Ha Lee, Department of Chemical Engineering, Yonsei University, 134 Shinchon-dong, Seodaemun-gu, Seoul 120-749, Korea; Fax: +82-2-312-6401; E-mail: leech@yonsei.ac.kr.

DOI: 10.1081/SS-200026757 0149-6395 (Print); 1520-5754 (Online)

packed bed showed a dependency on the flow rate and temperature of hot nitrogen. A dimensionless correlation of Nu_{PM}, Re_{PM}, and Pr was obtained from the experimental results, and the relation between Nu_{PM} and Re_{PM} in the correlation was similar to that derived from an internal flow in the vacant bed. Using the values of heat-transfer coefficients estimated from the thermal swing experiments, the dynamics of thermal regeneration in the zeolite 13X bed saturated with water was well predicted.

Key Words: Adsorption; Thermal regeneration; Heat-transfer coefficient; Zeolite 13X; Hot nitrogen.

INTRODUCTION

Thermal swing adsorption (TSA) is most commonly used to prevent air contamination from organic solvents of low concentration and to dehumidify gases. Specifically, air-drying by TSA is one of the major commercial gas separation processes.

One of the important factors in the simulation of the pressure swing adsorption (PSA) process is the accurate prediction of the pressure profile inside the bed at each step of a cycle. This is because the driving force of adsorption and desorption in a PSA process is the difference in the equilibrium adsorption amount or sorption rate with change of pressure.[1,2] In contrast, since TSA process is operated by varying the equilibrium adsorption amount with change of temperature, accurate prediction of the temperature profile inside the bed is more important in TSA than in PSA.

Since the thermal regeneration step of the a TSA process requires a great deal of energy to heat the bed, it is very important to estimate the thermal dynamics of that step accurately in evaluating the economic efficiency of the process. In that step, the heat of adsorption, the thermal properties of adsorbates and adsorbents, and heat transfer through the column wall can affect the temperature profile inside the bed. In particular, heat transfer through the wall should be taken into account unless an adiabatic condition can be guaranteed by eliminating heat transfer through the wall. Compared to simulation of PSA, it is expected that more rigorous models, as well as precise values of heat-transfer coefficients, should be used to predict accurately the thermal dynamics in the bed in TSA processes.

To predict the thermal dynamics in the bed, it is necessary that experiments and simulations should be performed to estimate the heat-transfer coefficients in the bed. Schork and Fair[3] estimated the heat-transfer coefficients at the inner and outer walls by matching the temperature profile measured in thermal swing of a fixed bed to their model. Using the heat-transfer coefficients, they simulated the adsorption and the thermal regeneration of ethane

and propane from carrier gas in an activated carbon bed. However, in their study, the same numerical values of heat-transfer coefficients at the inner and outer walls were applied to all the simulations, regardless of variations in the operating conditions. Moreover, the effect of each heat-transfer coefficient on the thermal dynamics in the fixed bed was barely described.

In the engineering plastic/resin and pharmaceutical industries, small-scale, air-drying TSA processes with zeolite are widely used to produce dry air with an extremely low dew point. In this process, hot nitrogen is generally used as the purge gas in the thermal regeneration step. In this study, the thermal dynamics in a near-adiabatic bed packed with zeolite 13X were investigated by applying hot nitrogen in a fixed bed. The heat-transfer coefficients in the fixed bed were obtained by matching the experimental temperature profile to the proper model. In the simulation of hot nitrogen regeneration, the thermally homogeneous model was compared with the thermally heterogeneous model, which is a more rigorous model, to investigate the validity of a simple energy balance for the thermal regeneration step. In addition, the dependency of each heat-transfer coefficient on the operating conditions of hot nitrogen regeneration was studied. The heat-transfer coefficients, estimated in hot nitrogen regeneration, were applied to predict the performance of a fixed bed saturated with water.

MATHEMATICAL MODEL

In this work, heterogeneous and homogeneous models were developed to describe the thermal dynamics in heating a clean bed using hot nitrogen. Using both mathematical models, several heat-transfer coefficients were obtained from experiments and then used for the simulation of thermal regeneration. The nonisothermal and nonadiabatic mathematical model used for the thermal regeneration was similar to that in previous studies.[4,5] To clarify the effect of two different thermal dynamic models, i.e., the heterogeneous and homogeneous models, on the dynamics of thermal regeneration, the simulation results of the regeneration by both models were compared.

Heterogeneous Model

The assumptions inherent in the heterogeneous model are as follows: (i) The flow pattern can be described by an axially dispersed plug flow model. (ii) The gas phase behaves as an ideal gas mixture. (iii) Axial conduction in the column wall can be neglected. (iv) Radial temperature gradients in the adsorption bed are negligible. (v) Pressure drop along the bed is neglected. These assumptions were widely accepted by researches in several studies.[1,6]

In this model, however, thermal equilibrium between the gas and adsorbed phases was not approached instantaneously.

The energy balance in the gas phase was expressed by the following equations:

$$-k_{ez}\frac{\partial^2 T_g}{\partial z^2}+\alpha\rho_g C_{Pg}\frac{\partial T_g}{\partial t}+\rho_g C_{Pg}\varepsilon u\frac{\partial T_g}{\partial z}+h_s a_s(1-\varepsilon)(T_g-T_s)+\frac{2h_i}{R_{Bi}}(T_g-T_w)=0 \tag{1}$$

$$\rho_p C_{Ps}\frac{\partial T_s}{\partial t}-h_s a_s(T_g-T_s)=0 \tag{2}$$

Liu and Ritter[7] suggested cubic temperature dependence to predict the heat capacity of gas in simulating the PSA process for solvent vapor recovery. The same cubic equation was used in estimating the heat capacity of nitrogen.[8]

In this study, the adsorption bed was wrapped with glass wool to keep the heat from being emitted through the wall of the adsorption bed while being heated with hot nitrogen. Nevertheless, since heat loss through the column wall and heat accumulation in the wall were not negligible, the column wall could not be assumed to be adiabatic. Therefore, another energy balance in the column wall was used as follows:

$$\rho_w C_{pw} A_w\frac{\partial T_w}{\partial t}=2\pi R_{Bi}h_i(T_g-T_w)-2\pi R_{Bo}h_o(T_w-T_{atm}) \tag{3a}$$

$$A_w=\pi(R_{Bo}^2-R_{Bi}^2) \tag{3b}$$

Due to the flange effect, which is similar to the effect of a fin, the temperature of hot nitrogen flowing into the bed became lower than the temperature of hot nitrogen produced in the heating system. In view of this effect, the value of R_{Bo} was recalculated at the entrance of hot nitrogen flow as a boundary condition:

$$\left.\frac{R_{Bo}}{A_w}\right|_{z=L}=\frac{\pi R_F+\pi\eta(R_F^2-R_{Bi}^2)}{\pi t_F(R_F^2-R_{Bi}^2)} \tag{4}$$

The boundary condition at the exit of hot nitrogen flow could be written by

$$\left.\frac{\partial T}{\partial z}\right|_{z=0}=0 \tag{5}$$

The initial condition for thermal swing became:

$$T(0,\ z)=T_{atm} \tag{6}$$

These equations were transformed into dimensionless equations by using the following dimensionless variables and parameters.

$$\tau = \frac{u_0 t}{L},\quad \zeta = \frac{z}{L},\quad \Theta_w = \frac{T_w}{T_f},\quad \Theta_g = \frac{T_g}{T_f},\quad \Theta_s = \frac{T_s}{T_f},\quad U = \frac{u}{u_0} \tag{7}$$

$$Pe_h = \frac{u_0 L \varepsilon \rho_g C_{Pg}}{k_{ez}} = \frac{\varepsilon \pi R_{Bi}^2 u_0 \rho_g C_{Pg}}{\pi R_{Bi}^2 k_{ez}/L}$$

$$= \frac{\text{Heat transfer by forced convection}}{\text{Heat transfer by effective thermal conduction}} \tag{8}$$

$$B = \frac{\alpha \rho_g C_{Pg} + \rho_B C_{Ps}}{\varepsilon \rho_g C_{Pg}} \tag{9}$$

$$D = \frac{2 h_i L}{R_{Bi} u_0 \varepsilon \rho_g C_{Pg}} = \frac{2\pi R_{Bi} L h_i}{\varepsilon \pi R_{Bi}^2 u_0 \rho_g C_{Pg}}$$

$$= \frac{\text{Heat transfer by thermal conduction at the inner wall}}{\text{Heat transfer by forced convection}} \tag{10}$$

$$E = \frac{\rho_w C_{Pw} A_w}{\varepsilon \rho_g C_{Pg} \pi R_{Bi}^2} \tag{11}$$

$$F = \frac{2 R_{Bo} h_o L}{u_0 \varepsilon \rho_g C_{Pg} R_{Bi}^2} = \frac{2\pi R_{Bo} h_o L}{\varepsilon \pi R_{Bi}^2 u_0 \rho_g C_{Pg}}$$

$$= \frac{\text{Heat transfer by thermal conduction at the outer wall}}{\text{Heat transfer by forced convection}} \tag{12}$$

$$I = \frac{h_s a_s L (1-\varepsilon)}{u_0 \varepsilon \rho_g C_{Pg}} = \frac{\text{Heat transfer from fluid to particle}}{\text{Heat transfer by forced convection}} \tag{13}$$

$$J = \frac{\rho_P C_{Ps} (1-\varepsilon)}{\rho_g C_{Pg} \varepsilon} \tag{14}$$

The resulting dimensionless forms of Eqs. (1–3) were as follows:

$$-\frac{1}{Pe_h}\frac{\partial^2 \Theta_g}{\partial \zeta^2} + \frac{\alpha}{\varepsilon}\frac{\partial \Theta_g}{\partial \tau} + U\frac{\partial \Theta_g}{\partial \zeta} + I(\Theta_g - \Theta_s) + D(\Theta_g - \Theta_w) = 0 \tag{15}$$

$$J\frac{\partial \Theta_s}{\partial \tau} - I(\Theta_g - \Theta_s) = 0 \tag{16}$$

$$E\frac{\partial \Theta_w}{\partial \tau} - D(\Theta - \Theta_w) + F(\Theta_w - \Theta|_{T_{atm}}) = 0 \tag{17}$$

The boundary and initial conditions, Eqs. (5) and (6), were converted into the following dimensionless forms:

$$\left.\frac{\partial \Theta}{\partial \zeta}\right|_{\zeta=0} = 0 \tag{18}$$

$$\Theta(0,\ \zeta) = \Theta|_{T_{\text{atm}}} \tag{19}$$

Homogeneous Model

In contrast to the heterogeneous model, it was assumed that the thermal equilibrium between the gas and adsorbed phases could be approached instantaneously. In this case, the following energy balance inside the bed was constructed without the division of the gas and solid phases.

$$-k_{\text{ez}}\frac{\partial^2 T}{\partial z^2} + (\alpha\rho_{\text{g}}C_{\text{Pg}} + \rho_{\text{B}}C_{\text{Ps}})\frac{\partial T}{\partial t} + \rho_{\text{g}}C_{\text{Pg}}\varepsilon u\frac{\partial T}{\partial z} + \frac{2h_{\text{i}}}{R_{\text{Bi}}}(T - T_{\text{w}}) = 0 \tag{20}$$

The same relation as the heterogeneous model was used to express the dependence of the heat capacity of nitrogen on temperature. Also, Eq. (3) was used as the energy balance in the wall.

Equation (20) was converted into the following dimensionless equation by using a new dimensionless parameter in addition to Eqs. (7–14)

$$\Theta = \frac{T}{T_{\text{f}}} \tag{21}$$

$$-\frac{1}{Pe_{\text{h}}}\frac{\partial^2 \Theta}{\partial \zeta^2} + B\frac{\partial \Theta}{\partial \tau} + U\frac{\partial \Theta}{\partial \zeta} + D(\Theta - \Theta_{\text{w}}) = 0 \tag{22}$$

The flange effect at the entrance of flow and the boundary and initial conditions were the same as in the heterogeneous model in Eqs. (4), (18), and (19).

Simulation

In this study, the dimensionless PDEs representing the energy balances with proper initial and boundary conditions were reduced to a set of ordinary differential equations (ODEs) by the method of lines. A first-order downward difference scheme and a second-order central difference scheme were used to approximate first-order and second-order spatial derivatives, respectively.[4] This numerical method was able to resolve first-order temporal and

second-order spatial hyperbolic partial differential equations with a substantial reduction in numerical oscillation and diffusion. Then, the final set of ODEs was solved by using the DASSL.

EXPERIMENT

Nitrogen was used as the carrier gas in the adsorption breakthrough tests and as hot purge gas in the thermal swing and the thermal regeneration breakthrough tests. The zeolite 13X (Sigma-Aldrich Korea Ltd, Yong-In, Korea) was used as an adsorbent. Before the experiment, zeolite 13X was regenerated for more than 12 hours at 593 K. The adsorption bed was made of a stainless steel pipe with a length of 30 cm, 3.3 cm ID, and 0.23 mm wall thickness. Five J-type thermocouples were installed at the position of 5, 10, 15, 20, and 25 cm from the bottom of the bed to measure the temperature inside the bed. The bed was wrapped with glass wool to prevent heat loss from the column wall. The physical properties of zeolite 13X and the characteristics of the adsorption bed were presented in detail in a previous study.[4] A schematic diagram of the experimental apparatus is shown in Fig. 1.

In the thermal swing experiment, the adsorption bed was packed with thermally regenerated zeolite 13X pellets. After the temperature of the adsorption bed decreased to room temperature, hot nitrogen was introduced and flowed downward through the bed. A tubular heater and a heating tape were used to produce hot purge gas at the desired temperature. Two J-type thermocouples were installed between the adsorption bed and the tubular heater to control the temperature of the hot nitrogen. Both a rotameter (Dwyer, RMA-23-SSV, Michigan, USA) and a wet test meter (Shinagawa, W-NK-1B, Tokyo, Japan) measured the flow rate of the nitrogen.

In the adsorption breakthrough experiments, water produced from an ultrapure system (Barnstead, D4641, Dubuque, USA) was used as a feed. A self-made humidity controller generated humidified gas with the desired relative humidity. Liquid water was injected into the nitrogen flow through a solenoid valve that was controlled by an in situ hygrometer (VAISALA, HMD40U, Tokyo, Japan). A heating tape was placed on the vapor-generating line to protect the generated humidified gas from condensation, and a precalibrated mass flow controller (Bronkhorst High-Tech, F-201C, Ruurlo, Netherlands) controlled the feed flow rate. The feed mixture flowed upward in the adsorption column. The final feed temperature and relative humidity were measured by another hygrometer located near the bottom of the bed. The effluent gas was also monitored by both a hygrometer (VAISALA, HMD40U) and a dew-point meter (Panametrics, MMS 35, Waltham, USA) located above the top of the bed. After the adsorption breakthrough experiment was finished, hot nitrogen

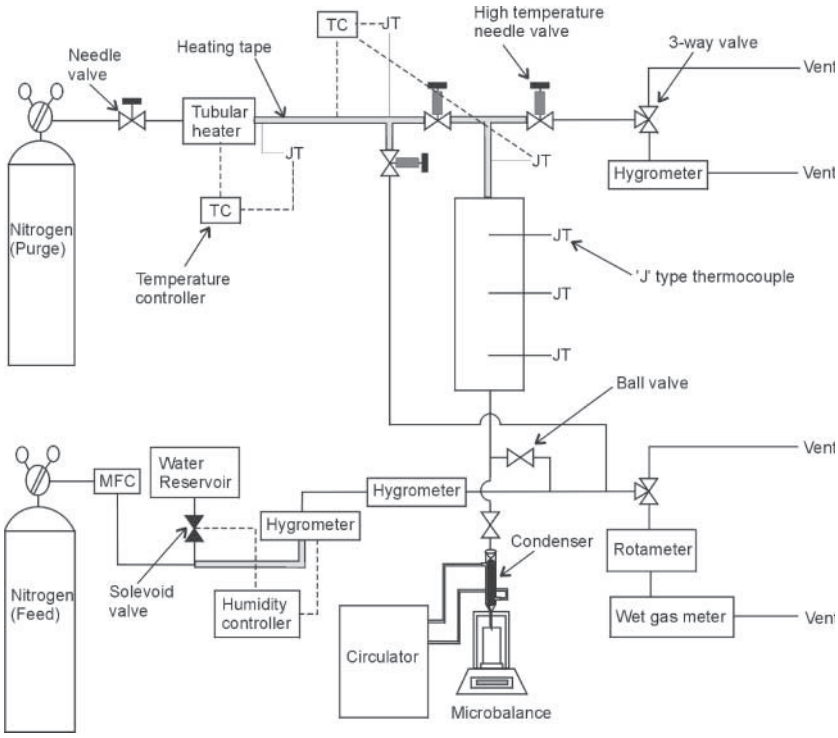

Figure 1. Schematic diagram of the apparatus of breakthrough experiment.

flowed into the top of the bed to thermally regenerate the adsorption bed. In the thermal regeneration experiment, hot nitrogen flow was produced in the same way as in the thermal swing experiment. The effluent from the adsorber was condensed by a heat exchanger and the amount of the condensed liquid was measured in real time with a microbalance. All the experimental data, such as time, temperature, pressure, feed flow rate, humidity, and mass, were stored on a computer.

To determine values of the heat-transfer coefficients, the thermal swing experiments were performed at flow rates of 14, 26, and 45 LSTP/min and at two different nitrogen temperatures, 473 and 423 K. The operating conditions in thermal swing experiments are listed in Table 1. The adsorption breakthrough experiment was performed under a feed condition of 12,740 ppm water concentration (54% relative humidity at 293 K), 9 LSTP/min feed flow rate, and 295 K ambient temperature. The corresponding regeneration experiment was performed under conditions of 473 K regeneration temperature, 26 LSTP/min purge flow rate, and 293 K ambient temperature.

Table 1. Experimental conditions of thermal swing experiments.

Run number	Temperature (K)			Flow rate (LSTP/min)
	T_{ini}	T_{atm}	T_f	
HT1	308	298	473	26
HT2	303	290	473	14
HT3	298	303	473	45
HT4	293	293	423	26

RESULTS AND DISCUSSION

Comparison of the Heterogeneous Model to the Homogeneous Model

In this study, thermal dynamics in an adsorbent bed were determined by four kinds of heat-transfer coefficients using the heterogeneous model mentioned previously. Among these coefficients, the heat-transfer coefficients at the inner and outer walls, h_i and h_o, were estimated by applying the heterogeneous model to the experimental temperature profile. However, the effective axial thermal conductivity, k_{ez}, and the heat-transfer coefficient between particle and fluid, h_s, were calculated using the following equations.

The effective axial thermal conductivity, k_{ez}, was calculated using the following empirical correlation.[9–11]

$$\frac{k_{ez}}{k_g} = \frac{k_e}{k_g} + \delta PrRe_p \tag{23a}$$

$$\frac{k_e}{k_g} = \varepsilon + \frac{1-\varepsilon}{\phi + (2/3)(k_g/k_s)} \tag{23b}$$

$$\phi = \phi_2 + (\phi_1 - \phi_2)\left(\frac{\varepsilon - 0.26}{0.216}\right) \quad \text{for} \quad 0.26 \le \varepsilon \le 0.476 \tag{23c}$$

where k_{ez}/k_g is 7.5 and δ is 0.64.

The following equation was used to estimate the heat-transfer coefficient between particle and fluid in the fixed bed.[10]

$$Nu_p = \frac{h_s D_p}{k_g} = Nu_0 + \left(\frac{1.15}{\varepsilon^{1/2}}\right) Pr^{1/3} Re_p^{1/2} \tag{24}$$

In Eq. (24), the limiting Nusselt number, Nu_0, in beds of active sphere is 10.5 using the analogy between the limiting Nusselt number and the limiting

Sherwood number.[10] In the experimental conditions, D_p is 0.3 cm and ε is 0.374. The other physical properties and flow conditions are shown in Table 2.

Figure 2 shows the experimental temperature profiles inside the bed at run #HT1 and the corresponding simulated results using the heterogeneous and homogeneous models. As shown in Fig. 2, both models predicted the experimental temperature profiles well. Furthermore, there was little difference between the temperature profiles predicted by the two models. The parameters, k_{ez} and h_s, were calculated from Eqs. (23) to (24) and the parameters, h_i and h_o, were estimated by fitting the experimental data to the model. All the parameters used in the simulation are listed in Table 3 with the experimental condition.

In the case of run #HT2, in Fig. 3, all the conditions were the same as those at run #HT1 except for the flow rate. Since the flow rate of the hot nitrogen changed from 26 to 14 LSTP/min, the temperature increase rate and the maximum temperature of each point in the bed were lower than those in Fig. 2. Since the variation of the flow rate resulted in the change of the corresponding Reynolds numbers in the bed, new values of k_{ez} and h_s were calculated from Eqs. 23–24. However, because the value of h_o appeared to have little or no relation to the flow rate of the hot nitrogen, it was kept constant regardless of the flow rate, i.e., between run #HT2 and run #HT1. On the

Table 2. Physical properties and flow conditions of nitrogen at several temperatures.

	Temperature (K)		
	473	423	Unit
Specific heat capacity (C_p)[a]	2.53×10^{-1}	2.51×10^{-1}	cal/g K
Viscosity (μ)[a]	2.58×10^{-4}	2.43×10^{-4}	g/cm sec
Thermal conductivity (k_g)[a]	8.84×10^{-5}	8.12×10^{-5}	cal/cm sec K
Density (ρ_g)[a]	7.93×10^{-4}	8.87×10^{-4}	g/cm^3
Prandtl number ($Pr = C_p\mu/k_g$)	0.738	0.751	—
Interstitial velocity (u_0) at flow rate	105 (14) 195 (26) 338 (45)	175 (26)	cm/sec (LSTP/min)
Reynolds number (Re_p) at flow rate	97.1 at 14 181 at 26 311 at 45	191 at 26	—
Reynolds number (Re_{PM}) at flow rate	58.0 at 14 108 at 26 186 at 45	114 at 26	—

[a]These values were obtained from Ref.[8]

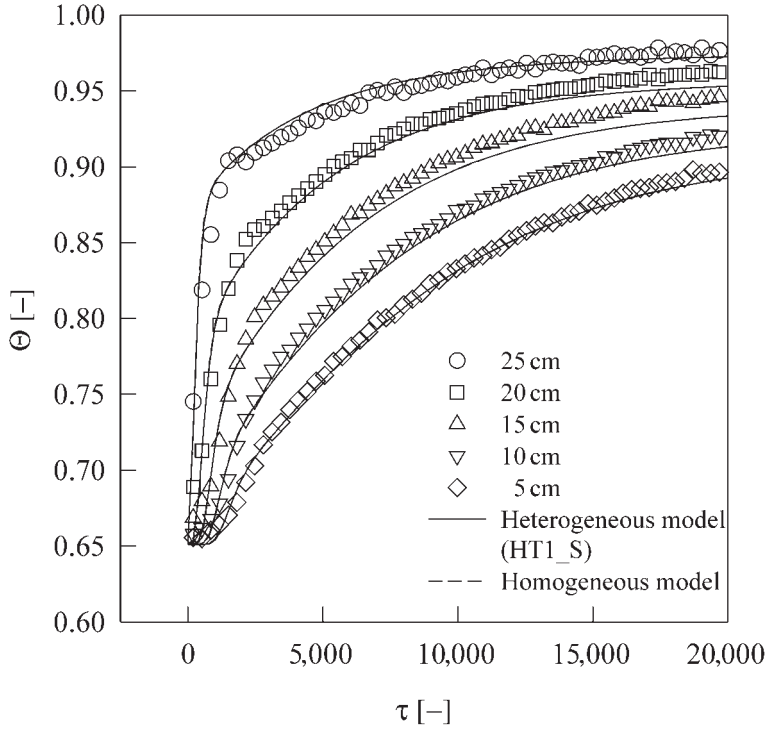

Figure 2. Comparison of the heterogeneous to the homogeneous models in the prediction of thermal swing experiment of run #HT1.

other hand, the h_i was estimated by matching the experimental data to the heterogeneous model. The value of h_i, the heat-transfer coefficient at the inner wall, in #HT2_S1 (Table 3) was $6.10 \times 10^{-4}\,\mathrm{cal/cm^2\,sec\,K}$, which was smaller than $1.00 \times 10^{-3}\,\mathrm{cal/cm^2\,sec\,K}$ estimated in #HT1_S. Furthermore, considering the effect of the value of h_s, the heat-transfer coefficient between gas and adsorbed phases, on the simulated result of the heterogeneous model, there were insignificant differences from that of the homogeneous model in Fig. 3, which was similar to the result in Fig. 2.

The simulated result in #HT2_S1 was compared with several different simulation cases to investigate the effect of each parameter on the prediction of thermal dynamics in Fig. 4. All the values of the parameters used in each simulation run are listed in Table 4. In simulation #HT2_S2, the value of h_i estimated in #HT1_S at the higher flow rate condition was used, but the others were the same as in #HT2_S1. In the case of #HT2_S3, the value of h_s taken from #HT2_S1 was replaced by the value of h_s from #HT1_S.

Table 3. Values of the parameters used in the simulations of thermal swing experiments.

Simulation run number[a]	Temperature (K)	Flow rate (LSTP/min)	k_{ez} (cal/cm sec K)	h_s (cal/cm^2 sec K)	h_i (cal/cm^2 sec K)	h_o (cal/cm^2 sec K)	Pe_h	I	D	F
HT2_S1	473	14	4.70×10^{-3}	8.00×10^{-3}	6.10×10^{-4}	1.00×10^{-4}	50.4	380	2.81	0.600
HT1_S	473	26	8.18×10^{-3}	9.80×10^{-3}	1.00×10^{-3}	1.00×10^{-4}	53.8	251	2.48	0.323
HT3_S1	473	45	1.36×10^{-2}	1.20×10^{-2}	1.55×10^{-3}	1.00×10^{-4}	56	178	2.22	0.187
HT4_S	423	26	8.06×10^{-3}	9.24×10^{-3}	1.05×10^{-3}	1.00×10^{-4}	54.2	238	2.62	0.325

[a]HT#_S# is an associated simulation for HT# in Table 1.

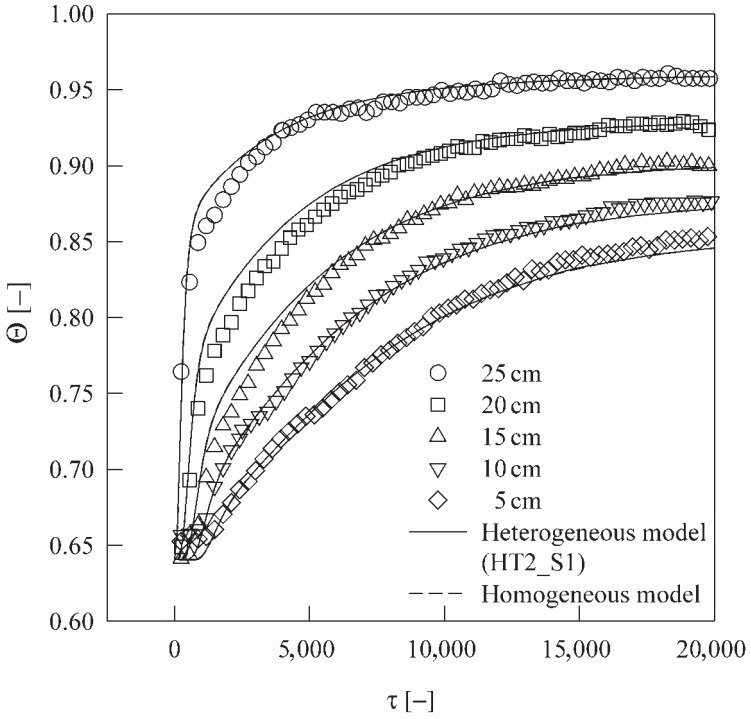

Figure 3. Comparison of the heterogeneous to the homogeneous models in the prediction of thermal swing experiment of run #HT2.

The effect of k_{ez} was investigated in #HT2_S4 by using the value of k_{ez} from #HT1_S.

As shown in Fig. 4, there was no significant difference between the simulated results in #HT2_S3 and #HT2_S1. This was because the heat transfer from the gas phase to the particle (h_s) had a negligible effect on the overall thermal dynamics in the fixed bed. In the case of k_{ez}, the simulated temperature profiles of #HT2_S4 were slightly higher than those of #HT2_S1, but the change in the thermal dynamics by the variance of k_{ez} was negligible. However, the simulated result in #HT2_S2 showed a significant difference from that in #HT2_S1 (see Fig. 4). Therefore, it was concluded that the value of h_i had a greater influence on thermal dynamics than any other heat-transfer parameters in this study.

To confirm the above roles of heat-transfer parameters in the fixed bed, the effect of heat-transfer parameters on thermal dynamics was investigated in run #HT3 with the highest flow rate, 45 LSTP/min, as shown in Table 1.

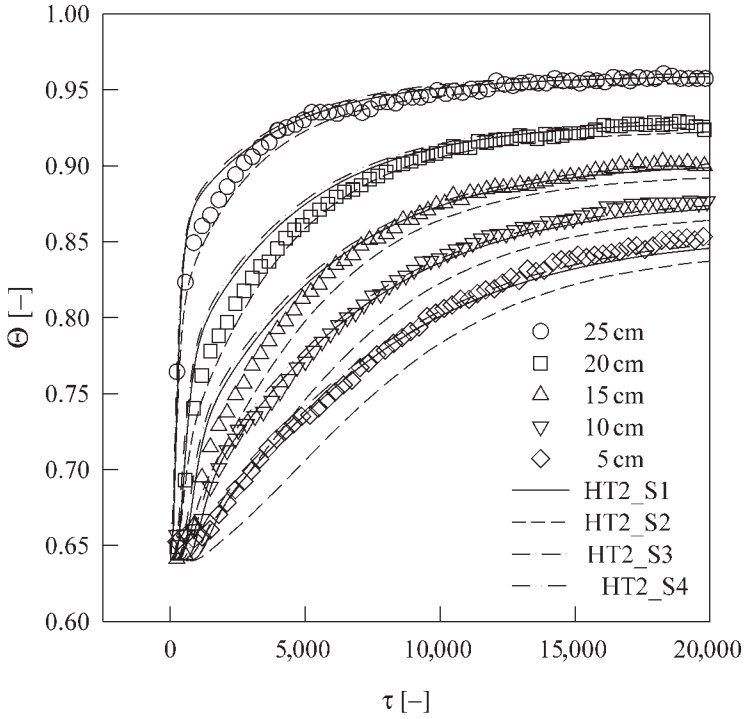

Figure 4. Effects of the parameters, h_i, h_s, and k_{ez}, on the temperature profile in the prediction of thermal swing experiment of run #HT2.

In simulation #HT3_S1, to predict the experimental result of run #HT3, the new h_s and k_{ez} were calculated according to Eqs. (23) and (24) and the value of h_o was the same as that in the simulation #HT1_S. The value of h_i in #HT3_S1 was 1.55×10^{-3} cal/cm^2 sec K, obtained from matching the experimental data to the model in Fig. 5. The value of h_i was higher than 1.00×10^{-3} cal/cm^2 sec K in the simulation #HT1_S, as shown in Table 3.

The simulated result of #HT3_S1 was compared with several simulation cases that had a different heat-transfer parameter in Table 4. Similar to the result in Fig. 4, the change of k_{ez} and h_s in #HT3_S3 and #HT3_S4 did not show any significant difference from that of #HT3_S1, even though the values of h_s and k_{ez} obtained from the different flow rate (#HT1_S) were used for the prediction. However, the simulated temperature profiles of #HT3_S2 were much higher than those of #HT3_S1. This implied that a higher value of h_i should be used as the flow rate increased. Also, the simulated result of the homogeneous model did not show any difference from

Table 4. Values of the parameters used in the simulations of the thermal swing in Figs. 4 and 5.

Simulation run number[a]	k_{ez} (Pe_h)	h_s (I)	h_i (D)	h_o (F)
473 K and 14 LSTP/min (run #HT2)				
HT2_S1	4.70×10^{-3} (50.4)	8.00×10^{-3} (380)	6.10×10^{-4} (2.81)	1.00×10^{-4} (0.600)
HT2_S2	4.70×10^{-3} (50.4)	8.00×10^{-3} (380)	1.00×10^{-3} (4.60)	1.00×10^{-4} (0.600)
HT2_S3	4.70×10^{-3} (50.4)	9.80×10^{-3} (466)	6.10×10^{-4} (2.81)	1.00×10^{-4} (0.600)
HT2_S4	8.18×10^{-3} (28.9)	8.00×10^{-3} (380)	6.10×10^{-4} (2.81)	1.00×10^{-4} (0.600)
473 K and 45 LSTP/min (run #HT3)				
HT3_S1	1.36×10^{-2} (56.0)	1.20×10^{-2} (178)	1.55×10^{-3} (2.22)	1.00×10^{-4} (0.187)
HT3_S2	1.36×10^{-2} (56.0)	1.20×10^{-2} (178)	1.00×10^{-3} (1.43)	1.00×10^{-4} (0.187)
HT3_S3	1.36×10^{-2} (56.0)	9.80×10^{-3} (145)	1.55×10^{-3} (2.22)	1.00×10^{-4} (0.187)
HT3_S4	8.18×10^{-3} (93.0)	1.20×10^{-2} (178)	1.55×10^{-3} (2.22)	1.00×10^{-4} (0.187)

[a]HT#_S# is an associated simulation for HT# in Table 1.

that of the heterogeneous model, #HT3_S1, as shown by the results in Figs. 2 and 3.

From these results, while h_o, h_s, and k_{ez} obtained from one flow rate condition could be reasonably used for the prediction of thermal dynamics at different flow rates, different values of h_i should be applied to the simulation to predict the thermal dynamics at different flow rates.

While the experimental runs #HT1, #HT2, and #HT3 were performed to investigate the effect of flow rate on thermal dynamics in the fixed bed, the effect of the temperature of hot nitrogen was studied in run #HT4. Figure 6 shows the experimental results of run #HT4, in which the temperature of hot nitrogen was decreased to 423 K from 473 K, as shown in Table 1. Also, the experimental results of #HT4 are compared with the simulation #HT4_S and all the heat-transfer parameters used in #HT4_S are listed in Table 3. The value of h_i estimated in #HT4_S was a little greater than that estimated in #HT1_S, as shown in Table 3. However, the difference in the estimated h_i values between the two operating conditions was very small in

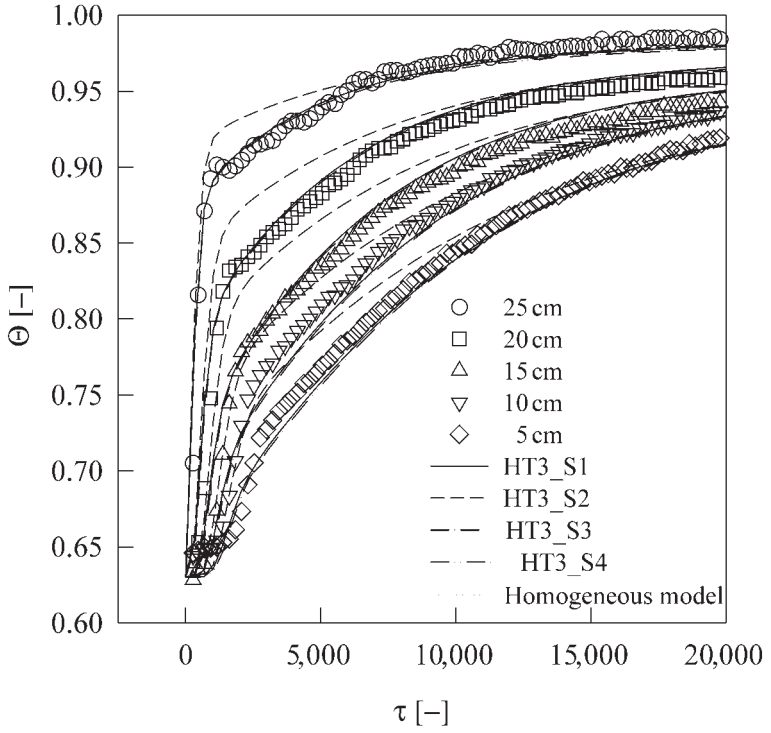

Figure 5. Comparison of the heterogeneous to the homogeneous models and effects of the parameters, h_i, h_s, and k_{ez}, on the temperature profile in the prediction of thermal swing experiment of run #HT3.

spite of the temperature difference of 50 K. It meant that the effect of the flow rate of nitrogen was more important in predicting the thermal dynamics than the effect of the temperature of nitrogen in this experimental range.

To clearly present the robustness of the parameters between the experiment and simulation, the following equation was applied for averaged-percentage deviation, $\Delta\Theta$:

$$\Delta\Theta(\%) = \frac{100}{k}\sum_{j=1}^{k}\left|\frac{\Theta_j^{\exp} - \Theta_j^{\text{sim}}}{\Theta_j^{\exp}}\right| \tag{25}$$

The values of $\Delta\Theta$ calculated at each location of the bed is presented in Table 5.

As mentioned before, there is little difference between the results by the heterogeneous model and the homogeneous model. However, in case of

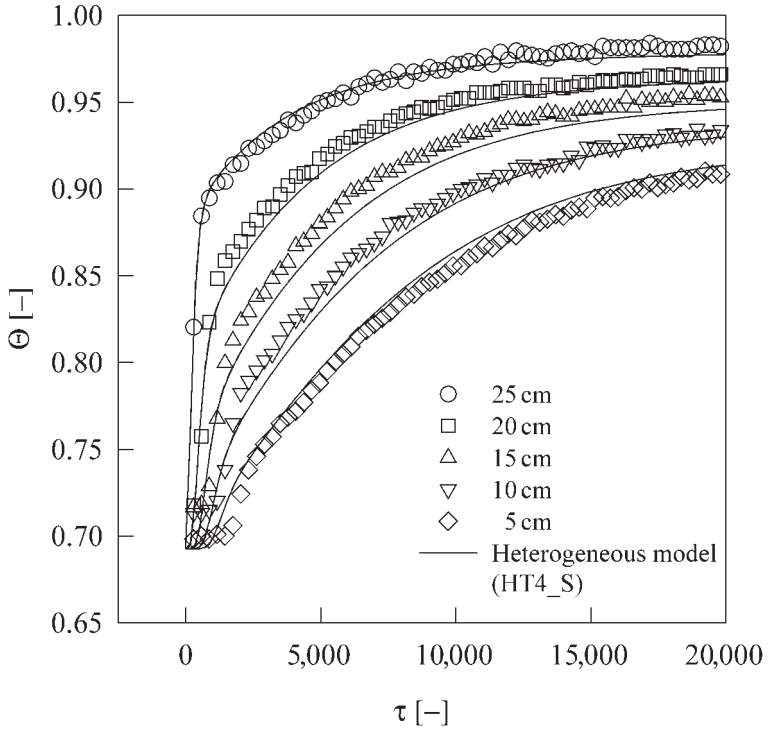

Figure 6. Prediction of thermal swing experiment of run #HT4 by heterogeneous model.

the heterogeneous model, the results of $\Delta\Theta$ in both #HT2_S2 and #HT3_S2 were higher than the others. From these results, it is apparent that the value of h_i plays a key role in the prediction of thermal dynamics compared with any other heat-transfer parameters and showed relatively strong dependency on flow rate and temperature.

Parametric Study of Heat-Transfer Coefficients

It is important to elucidate the effect of each heat-transfer parameter on thermal dynamics through parametric study. Equations (8), (10), (12), and (13) represent the dimensionless form of each heat-transfer coefficient based on heat transfer by forced convection. The dimensionless values of the respective coefficients obtained from the experiment are listed in Table 4.

Table 5. Averaged-percentage deviation between experiment and simulation.

Simulation run number	Thermocouple location in the bed (cm)				
	25	20	15	10	5
473 K and 26 LSTP/min (run #HT1): (%)					
(Heterogeneous model)					
HT1_S	0.590	0.854	1.181	0.853	0.434
(Homogeneous model)	0.602	0.690	1.208	0.868	0.445
473 K and 14 LSTP/min (run #HT2): (%)					
(Heterogeneous model)					
HT2_S1	0.505	0.826	0.695	0.523	0.622
HT2_S2	0.591	0.634	1.359	2.377	2.699
HT2_S3	0.507	0.825	0.696	0.528	0.629
HT2_S4	0.735	1.190	0.896	0.577	0.584
(Homogeneous model)	0.515	0.818	0.690	0.533	0.633
473 K and 45 LSTP/min (run #HT3): (%)					
(Heterogeneous model)					
HT3_S1	0.506	0.980	0.942	0.948	0.852
HT3_S2	0.932	1.911	2.310	1.358	1.555
HT3_S3	0.502	0.981	0.944	0.946	0.852
HT3_S4	0.568	0.765	0.779	1.063	0.985
423 K and 26 LSTP/min (run #HT4): (%)					
(Heterogeneous model)					
HT4_S	0.372	0.795	1.101	0.857	0.916

Figure 7 shows the effects of Pe_h related with k_{ez} and I related with h_s on the thermal dynamics of thermal swing. The dimensionless group, Pe_h, refers to the ratio of heat transfer by forced convection to heat transfer by thermal conduction in the axial direction in Eq. (8). As the value of k_{ez} decreased, the value of Pe_h increased, and heat transfer by thermal conduction in the axial direction diminished. An increase of Pe_h led to a decrease of the temperature rise over the whole range of the simulation time, as shown in Fig. 7(a). Moreover, the effect of Pe_h was greater near the exit of flow than near the entrance of flow because the effect of the heat conduction accumulated along the flow direction. However, the difference among the temperature profiles caused by different values of Pe_h decreased with an increase of Pe_h.

Figure 7(b) represents the effect of the dimensionless group, I, on the thermal dynamics in the thermal swing of the fixed bed. As the value of

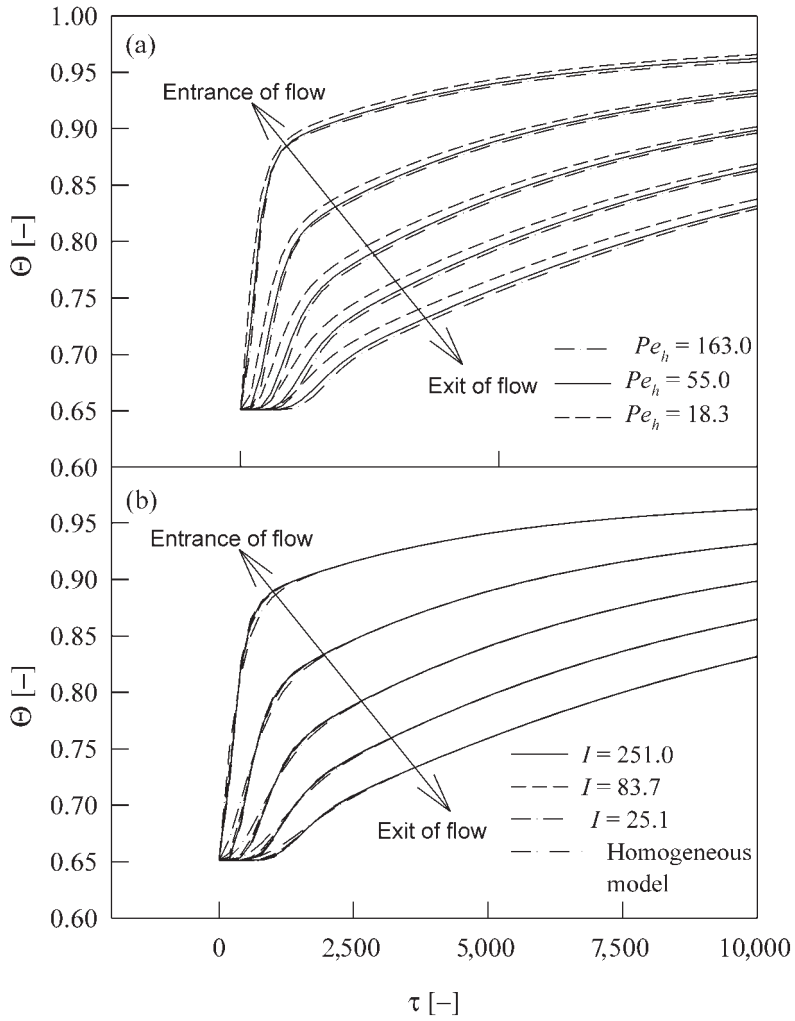

Figure 7. Effect of the dimensionless groups, (a) Pe_h and (b) I, on the temperature profile in thermal swing of the fixed bed. (a) Parameter: $I = 251$, $D = 2.48$, $F = 0.323$; (b) parameter: $Pe_h = 55.0$, $D = 2.48$, $F = 0.323$.

h_s became greater, the value of I increased and the heat transfer from fluid to particle grew larger. Therefore, as the dimensionless parameter, I, became large, the simulated result of the heterogeneous model became similar to that of the homogeneous model, as shown in Figure 7(b), i.e., because the gas and solid phases reached a continual thermal equilibrium. In the cases

of $I = 251.0$ and $I = 83.7$, the temperature near the exit began to increase after the temperature near the entrance of the hot nitrogen flow almost approached maximum. This was because the heat energy of hot nitrogen could approach the lower part of the bed after the upper part was adequately heated up. However, such thermal dynamic behavior was changed in the case of $I = 25.1$. In this case, the temperatures at all axial positions in the bed began to increase nearly simultaneously. Because the hot nitrogen passed the solid phase near the flow entrance without adequate heat transfer, it could reach the end of bed and still retain some excess heat. However, the parameter, I, affected the thermal dynamics only at the beginning and did not have significant effect on the thermal dynamics after a certain period of time had passed. Therefore, it could be concluded that the effect of h_s was important only at the initial time in the case of thermal regeneration breakthrough.

Figure 8 represents the effects of the dimensionless parameters, D related to h_i and F related to h_o, on the thermal dynamics of thermal swing. A variation of the value of D within the same order of magnitude could result in a great change of the temperature profile, as shown in Fig. 8(a). As D increased, the temperatures at the different bed axial positions approached the steady-state temperatures very slowly.

Meanwhile, for the dimensionless group, F, the thermal dynamics were very sensitive to a small variation in the range of the same order in Fig. 8(b). The effect of the value of F on the thermal dynamics in the early stages was negligible, while the steady-state temperature at each position of the bed was greatly affected by the value of F because the extent of the heat loss from the column wall to the surroundings depended on the F value. From the results, it can be seen that accurate prediction of the heat-transfer parameters for thermal conduction at the inner and outer walls of the bed was more important than the other parameters in the prediction of thermal dynamics at the fixed bed.

In the heat transfer of internal flow in a circular tube, the Nusselt number for fully developed and fully turbulent flow in the smooth tube, Nu, is given by:[12]

$$\mathrm{Nu} = 0.023 Re^{0.8} Pr^{n} \tag{26}$$

where $n = 0.5$ for $0.5 \leq Pr \leq 5.0$ and $n = 1/3$ for $Pr \geq 5.0$.

Although this correlation was derived from the internal flow in an empty tube, it was expected that there existed a similar relationship between the Nusselt and Reynolds numbers in the case of the heat transfer in the internal flow in the packed bed. As seen in the results of simulation #HT1_S, #HT2_S1, and #HT3_S1, the value of the estimated h_i increased as the

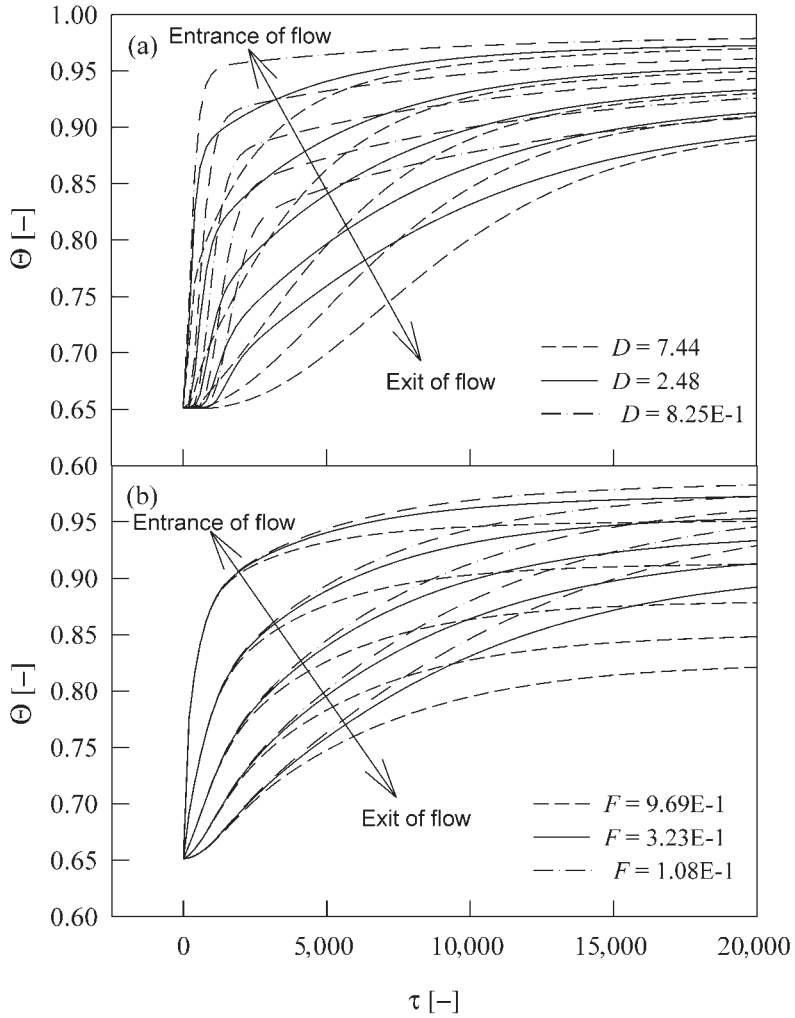

Figure 8. Effect of the dimensionless groups, (a) D and (b) F, on the temperature profile in thermal swing of the fixed bed. (a) Parameter: $Pe_h = 55.0.$, $I = 251$, $F = 0.323$; (b) parameter: $Pe_h = 55.0$, $I = 251$, $D = 2.48$.

flow rate increased. Furthermore, from the comparison of #HT1_S and #HT4_S, the value of the estimated h_i increased a little as the temperature of hot nitrogen decreased. Therefore, a dimensionless correlation modified from Eq. (26) could be developed for heat transfer in a fixed bed packed with porous media.

The Nusselt number, Nu_{PM}, and the Reynolds number, Re_{PM}, in the porous media were defined as follows:

$$Nu_{PM} = \frac{h_i D}{k_e} \tag{27}$$

$$Re_{PM} = \frac{D_p u_0 \rho \varepsilon}{\mu(1-\varepsilon)} \tag{28}$$

where u_o is constant interstitial velocity.

Since the diameter of the bed used in this study was so small that heat transfer in the radial direction could be assumed to be negligible, the effective thermal conductivity in the packed bed, k_e, could be used instead of the effective thermal conductivity in the radial direction.[13] The Prandtl number in the correlation was fixed at the average value of the Prandtl numbers obtained at 473 and 423 K, because the Prandtl number did not vary significantly in this experimental range compared with the Reynolds number in porous media, as shown in Table 2.

In Fig. 9, the following correlation of Nu_{PM} and Re_{PM} was developed for the internal flow of hot nitrogen gas through the packed bed.

$$Nu_{PM} = 0.00618 Re_{PM}^{0.8} Pr \tag{29}$$

It is interesting to note that the Nusselt number in the packed bed had the same dependency on the Reynolds number in porous media as that at the vacant pipe in Eq. (26).

Thermal Regeneration of the Water-Saturated Bed

On the basis of the results of the experimental and theoretical studies, it was concluded that the parameter, h_s, in the heterogeneous model did not have significant effect on the thermal dynamics of the fixed bed in this system. Therefore, the simulated result of the homogeneous model was quite similar to that of the heterogeneous model in the simulation of the thermal swing experiments.

To ascertain if this result could be applied to the thermal regeneration of the bed saturated with an adsorbate as well as simple heating of the clean bed, a thermal regeneration of the zeolite 13X bed saturated with water was studied experimentally and numerically. In this study, adsorption breakthrough was performed under the condition of 12,740 ppm water concentration (54% RH at 293 K) in the feed, 9 LSTP/min feed flow rate, and 295 K ambient temperature. After the adsorption bed was saturated at the feed concentration, thermal regeneration was performed with hot nitrogen at 473 K, a flow rate

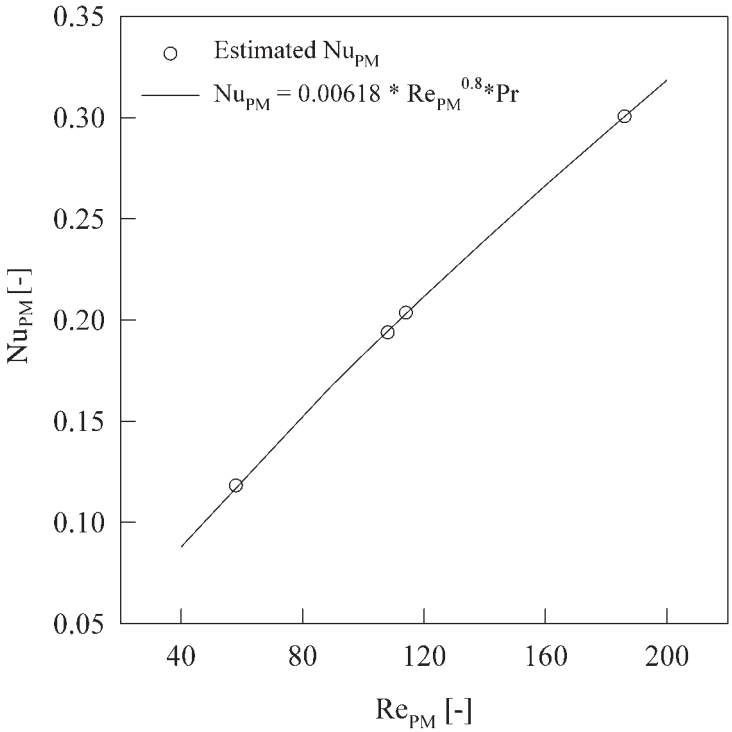

Figure 9. Correlation between Nu_{PM} and Re_{PM} for hot nitrogen flow in the fixed bed packed with zeolite 13X.

of 26 LSTP/min, and 295 K ambient temperature, i.e., the same as with run #HT1. Also, a nonisothermal and nonadiabatic model, taking into account either the thermally heterogeneous or homogeneous heat balance, was applied to predict thermal regeneration. The heat-transfer coefficients obtained from the previous thermal swing process were used in the simulation of the thermal regeneration experiment.

As shown in Fig. 10(a), the experimental temperature profiles were well predicted by the simulation using either the homogeneous model or the heterogeneous model with $h_s = 9.80 \times 10^{-3}\,\mathrm{cal/cm^2\,sec\,K}$, which was estimated from the simulation #HT1_S. In addition, there was no significant difference between the simulated results of the homogeneous model and the heterogeneous model in this case. However, if a very low value of $1.00 \times 10^{-4}\,\mathrm{cal/cm^2\,sec\,K}$ was used as h_s, instantaneous thermal equilibrium could not be reached, as shown in Fig. 10(a). In this case, the temperature in the gas phase at each axial position in the bed began to increase

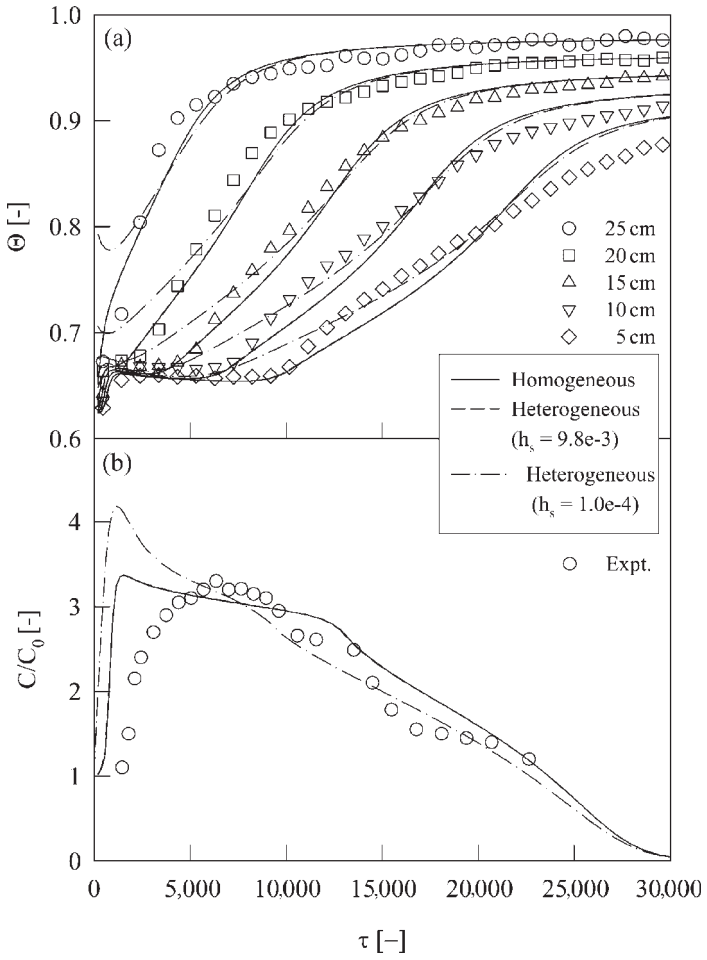

Figure 10. Comparison of the heterogeneous to the homogeneous models for (a) temperature profile and (b) effluent concentration in regeneration breakthrough. Adsorption condition: 12,740 ppm (54% RH at 293 K), 9 LSTP/min feed flow rate, 295 K ambient temperature. Regeneration condition: 473 K purge temperature, 26 LSTP/min purge flow rate, 295 K ambient temperature.

drastically and simultaneously at the initial regeneration time and then approached the steady-state temperature gradually. This implied that the hot nitrogen gas passed through the upper part of the bed without heating the solid phase sufficiently and could approach the end of the bed without much heat loss. Therefore, the amount of the desorbed water at the initial

regeneration time in the case of $h_s = 1.00 \times 10^{-4}\,\mathrm{cal/cm^2\,sec\,K}$ was higher than in the simulation case of $h_s = 9.80 \times 10^{-3}\,\mathrm{cal/cm^2\,sec\,K}$, as shown in Fig. 10(b).

As a result, in the prediction of thermal regeneration, the result of the homogeneous model is the same as that of the heterogeneous model, if h_s is well predicted by Eq. (24). Otherwise, the predictions of the heterogeneous and homogeneous models can show a difference in temperature and concentration profiles, especially at the early regeneration stage.

CONCLUSION

In simulating the thermal dynamics of TSA process, it is important to obtain precise heat-transfer coefficients in relation to thermal dynamics in the adsorption bed. In this study, the heat-transfer coefficients were estimated from the thermal swing experiments at a near-adiabatic bed packed with thermally regenerated zeolite 13X. Thermally heterogeneous and homogenous models were developed to simulate the thermal swing of the fixed bed.

With the exception of h_i and h_o, the variation of h_s and k_{ez} did not have a significant impact on predicting the thermal dynamics of thermal swing. Therefore, the values of h_s and k_{ez} obtained from one flow rate condition could be applied to predict the thermal dynamics of the other flow rate condition. Also, the value of h_o, which affected the steady-state temperature in the bed, was assumed to be constant because it was not related to the flow rate and the limited variation of temperature. However, since the value of h_i had a strong influence on thermal dynamics and showed a dependency on flow rate and temperature, it was important to estimate the value of h_i accurately. A correlation between Nu_{PM} and Re_{PM} to represent a dependency of h_i on flow rate and temperature of the hot nitrogen in an adsorption bed was presented in a similar form as a correlation derived from the internal flow in an empty tube.

The simulated result of a thermal swing using the heterogeneous model is the same as that using the homogeneous model if the value of h_s is estimated from a proper correlation. In addition, this value in the heterogeneous model could be applied to predict the thermal regeneration of a bed that was presaturated with strong adsorbate having high heat capacity. Even in this case, the simulated result of the heterogeneous model was very similar to that of the homogeneous model. However, if the estimated value of h_s was very low, the temperature and concentration profiles predicted by the heterogeneous model with the wrong value of h_s could show a significant disparity from those predicted by the homogeneous model at the outset of regeneration.

NOMENCLATURE

a_s	geometric surface area of spherical pellets (cm^{-1})
A	area (cm^2)
C	concentration (mol/cm^3)
C_p	heat capacity ($cal/g\,K$)
D	inner diameter of the bed (cm)
D_p	particle diameter (cm)
h_i	heat-transfer coefficient at the inner wall ($cal/cm^2\,sec\,K$)
h_o	heat-transfer coefficient at the outer wall ($cal/cm^2\,sec\,K$)
h_s	heat-transfer coefficient between gas and adsorbed phases ($cal/cm^2\,sec\,K$)
k_{ez}	effective axial thermal conductivity in the packed bed ($cal/cm\,sec\,K$)
k_e	effective thermal conductivity in the packed bed ($cal/cm\,sec\cdot K$)
k_g	thermal conductivity in the gas phase ($cal/cm\,sec\,K$)
L	length of adsorption bed (cm)
Nu	Nusselt number in the vacant pipe, h_iD/k_g
Nu_{PM}	Nusselt number in the porous media, h_iD/k_e
Pe_h	Peclet number in heat transfer, $u_0L\varepsilon\rho_gC_{pg}/k_{ez}$
Pr	Prandtl number, $C_p\mu/k_g$
Re	Reynolds number in the vacant pipe, $Du_0\rho_g/\mu$
Re_p	Reynolds number around the particle, $D_pu_0\rho_g/\mu$
Re_{PM}	Reynolds number in the porous media, $D_pu_0\rho_g\varepsilon/\mu(1-\varepsilon)$
t	time (sec) or thickness (cm)
t_F	axial length of flange (cm)
T	temperature (K)
u	interstitial velocity (cm/sec)
U	dimensionless interstitial velocity (cm/sec)
z	axial distance along adsorption bed (cm)

Greek Symbols

α	total void fraction
ε	bed void fraction
ϕ, ϕ_1, ϕ_2	parameters in Eqs. (23)
μ	viscosity ($g/cm\cdot sec$)
η	fin efficiency
ρ	density (g/cm^3)
ζ	dimensionless axial distance along the bed
Θ	dimensionless temperature

Subscripts

0	constant value
atm	atmospheric
B	bed
f	feed
F	flange
g	gas phase
i	inner
o	outer
p	pellet
w	wall

ACKNOWLEDGMENT

The financial support of the Korea Energy Management Corporation and the Korea Research Foundation (KRF-2001-005-E0031) are gratefully acknowledged.

REFERENCES

1. Yang, R.T. *Gas Separation by Adsorption Processes*; Butterworths: Boston, 1987.
2. Choi, W.-K.; Kwon, T.-I.; Yeo, Y.-K.; Lee, H.; Song, H.K.; Na, B.-K. Optimal operation of the pressure swing adsorption (PSA) process for CO_2 recovery. Korean J. Chem. Eng. **2003**, *20* (4), 617–623.
3. Schork, J.M.; Fair, J.R. Parametric analysis of thermal regeneration of adsorption beds. Ind. Eng. Chem. Res. **1988**, *27*, 457–469.
4. Ahn, H.; Lee, C.-H. Adsorption dynamics of water in layered bed for air-drying TSA process. AIChE J. **2003**, *49* (6), 1601–1609.
5. Ryu, Y.-K.; Lee, S.-J.; Kim, J.-W.; Haam, S.; Lee, C.-H. Adsorption equilibrium and kinetics of H_2O on zeolite 13X. Korean J. Chem. Eng. **2001**, *18* (4), 525–535.
6. Lee, C.-H.; Yang, J.; Ahn, H. Effects of carbon-to-zeolite ratio on layered bed H_2 PSA for coke oven gas. AIChE J. **1999**, *45* (3), 535–549.
7. Liu, Y.; Ritter, J.A. Evaluation of model approximations in simulating pressure swing adsorption-solvent vapor recovery. Ind. Eng. Chem. Res. **1997**, *36*, 1767–1778.
8. Reid, R.C.; Prausnitz, J.M.; Poling, B.E. *The Properties of Gases and Liquids*; McGraw-Hill: Singapore, 1988.

9. Kunii, D.; Smith, J.M. Heat transfer characteristics of porous rocks. AIChE J. **1960**, *6* (1), 71–78.
10. Suzuki, M. *Adsorption Engineering*; Elsevier: Amsterdam, 1990.
11. Yagi, S.; Kunii, D.; Wakao, N. Studies on axial effective thermal conductivities in packed beds. AIChE J. **1960**, *6* (4), 543–546.
12. Thomas, L.C. *Heat Transfer*; Prentice-Hall: 1992.
13. Kim, M.-B.; Moon, J.-H.; Lee, C.-H.; Oh, M.; Cho, W. Effect of heat transfer on the transient dynamics of TSA process. Korean J. Chem. Eng. **2004**, *21* (3), *in press*.